Chapter 4

Stabilization Control for the Giant Swing Motion of the Horizontal Bar Gymnastic Robot Using Delayed Feedback Control

Dasheng Liu

Additional information is available at the end of the chapter

http://dx.doi.org/10.5772/65831

Abstract

Open-loop dynamic characteristics of an underactuated system with nonholonomic constraints, such as a horizontal bar gymnastic robot, show the chaotic nature due to its nonlinearity. This chapter deals with the stabilization problems of periodic motions for the giant swing motion of gymnastic robot using chaos control methods. In order to make an extension of the chaos control method and apply it to a new practical use, some stabilization control strategies were proposed, which were, based on the idea of delayed feedback control (DFC), devised to stabilize the periodic motions embedded in the movements of the gymnastic robot. Moreover, its validity has been investigated by numerical simulations. First, a method named as prediction-based DFC was proposed for a two-link gymnastic robot using a Poincaré section. Meanwhile, a way to calculate analytically the error transfer matrix and the input matrix that are necessary for discretization was investigated. Second, an improved DFC method, multiprediction delayed feedback control, using a periodic gain, was extended to a four-link gymnastic robot. A set of plural Poincare maps were defined with regard to the original continuous-time system as a T-periodic discrete-time system. Finally, some simulation results showed the effectiveness of the proposed methods.

Keywords: gymnastic robot, nonholonomic system, giant swing motion, delayed feedback control, chaos control, stabilization

1. Introduction

In the past decades, scientists have found that unusual and unexpected evolution patterns arise frequently in numerous natural and model nonlinear systems in physics, chemistry, biology, engineering, medicine, economics, and so forth, since Lorenz [1] in 1963, May [2] in 1976, and others reported chaotic behavior in very simple dynamical models. The most peculiar aspect of these patterns is their random-like behavior, although the systems are deterministic, in other words, the deterministic nature of these systems does not make them predictable [3]. This behavior is known as deterministic chaos, or simply chaos. It is considered that chaos is due to sensitive dependence on the initial conditions. This property implies that two trajectories emerging from two different close-by initial conditions separate exponentially in the course of time. Due to this property, and due to the fact that, in general, experimental initial conditions are never known perfectly, chaotic systems cannot be predicted by their long-term behaviors.

This feature of their critical sensitivity to initial conditions, often regarded as a troublesome property, made chaos undesirable in engineering control practice, and most experimentalists considered such characteristics as something to be strongly avoided since it restricts the operating range of many electronic and mechanic devices. Besides that, chaotic systems exhibit two other important properties. One is that there is an infinite number of unstable periodic orbits embedded in the underlying chaotic set. The other is that the dynamics in the chaotic attractor is ergodic; that is to say, the system visits ergodically small neighborhood of every unstable fixed point during its temporal evolution [4].

Although the existence of steady states and an infinity of different unstable periodic orbits embedded in chaotic motion is not usually obvious in free-running chaotic evolution, these orbits offer a great potential advantage if one wants to control a chaotic system. The presence of chaos may be a great advantage for control in a variety of situations. In a nonchaotic system, small controls typically can only change the system dynamics slightly. However, in a chaotic system, one can choose between a rich variety of dynamical behaviors. It is then not surprising that the matter of controlling chaotic systems has come under detailed investigation by several different scientific communities. Chaotic dynamics consists of a motion where the system moves in the neighborhood of one of the unstable periodic orbits (UPO) for a while, then falls close to a different UPO and remains for a limited time. Thus, it allows to exploit a single dynamical system for the production of a large number of different periodic behaviors so that the single system can carry out different performances with different yields [5]. The result is to render an otherwise chaotic motion more stable and predictable, which is often an advantage. The perturbation must be tiny, to avoid significant modification of the system's natural dynamics.

Since Ott, Grebogi, and Yorke [6], in 1990, pointed out the existence of many unstable periodic orbits (UPOs) embedded in chaotic attractors that raise the possibility of using very small external forces to obtain various types of regular behavior, Pyragas [7] in 1992, proposed a

http://dx.doi.org/10.5772/65831

so-called "Delayed Feedback Control (DFC)" idea that an appropriate continuous controlling signal formed from the difference between the current state and the delayed state is injected into the system, whose intensity is practically zero as the system evolves close to the desired periodic orbit but increases when it drifts away from the desired orbit, several techniques were devised for controlling chaos [8–21] during the past years and applied to various systems [22–31]. It is worth noting that in spite of the enormous number of applications among the chaos control, very few rigorous results are so far available. Most results are justified by computer simulations rather than by analytical tools. Therefore, many problems remain unsolved.

On the other hand, recently in the field of mechanical and control engineering, the open-loop link mechanism, in terms of diversity and ease of movement, has been used in industrial robots, although a large control input is needed due to speeding up, and the opposing force to the joint and the base increases. Therefore, the actuator with a large driving performance is needed, and the mass of the entire mechanism is increased. It is thought that the control method using the opposing force and gravity is important to achieve the desired movement with high speed and high efficiency by the limited driving performance. The joint type movement robot is actively researched in recent years, and the achievement of dynamic walking and running with high speed and efficiency becomes a problem. Although living creatures, such as humans or animals, have achieved the high-speed movement by using the open-loop link mechanism, it is thought that this is because that a good movement possessing the energy efficiency and small joint drive power and small impact power, and so forth in the gravitational filed had been acquired adaptively during the process of evolution. For example, the human biped locomotion is performed by dynamic link mechanism coupled to the pendulum motion [32, 33], and brachiation (movement across branches) used by the monkeys is a specialized form of arboreal locomotion that can be seen as a continuous pendulum motion [34, 35]. In addition, humans have competed for the manipulation of their own multi-degree of freedom link mechanism through sports or physical exercise, and so forth, and the achievement of a complex movement meeting a specific initial terminal requirement as a technique.

The systems, such as humans and robots, which control the internal force to achieve motions by using reaction force from the outside world, can be modeled as an underactuated link mechanism. These systems usually have nonholonomic second-order constraints due to the presence of passive joints, which makes development of control methods a difficult task. In recent years, studies on underactuated mechanical systems that possess fewer actuators than degrees of freedom have received increased interest [36–40].

Open-loop dynamic characteristics of an underactuated system with nonholonomic constraints show the chaotic nature that even though there are small differences in the initial conditions, the amplitude grows to be a completely different movement for its nonlinearity due to centrifugal force, Coriolis force, and gravity. Motions control of underactuated systems known also as nonholonomic control, such as wheeled robot positioning control [41], aerial posture control of space robots [42], and positioning control of underactuated link mechanism robot [43, 44], have been studied. However, a generalized control method has not yet been

established to this kind of system due to the difficulties in analysis, and the fact that for an underactuated system, it cannot be directly controlled because of the generalized coordinates of its passive parts. Control methods, which utilize empirical skills catching the motion characteristics and proper motion of the system, are desirable. From the above-mentioned viewpoint, in order to achieve a robot with a high-speed, highly effective optimal motion, and the skill in movement seen in living creatures, fundamental researches on the control method and the trajectory planning method using periodic free movement for the linkage with a passive joint have been done [45–51].

The remaining parts of this chapter are organized as follows: Section 2 discusses a kind of DFC method, PDFC, for a two-link gymnastic robot by using of a Poincaré section. In the Section 3, an improved DFC method, Multiprediction Delayed Feedback Control, is extended to a four-link gymnastic robot. Section 4 gives some numerical simulations to show the effectiveness of the proposed method. Section 5 summarizes the chapter.

2. Delayed feedback control for a two-link horizontal bar gymnastic robot

The two-link horizontal bar gymnastic robot is a highly simplified model of a human gymnast on a high bar, where the underactuated first joint models the gymnast's hands on the bar and the actuated second joint models the gymnast's waist [52]. Studies on such underactuated mechanical systems that possess fewer actuators than degrees of freedom, as gymnastic robot with the underactuated first joint, have received considerable interest in recent years. Open-loop dynamic characteristics of such a linkage as this kind of system, which is classified as an underactuated systems with nonholonomic constraints, show the chaotic nature that even though there are small differences in initial conditions, the amplitude grows to be a completely different movement for its nonlinearity due to centrifugal force, Coriolis force, and gravity. Since a generalized control method has not yet been established to this kind of system for the difficulties in analysis, their control problems are challenging.

While applying the original DFC to the continuous system, such as gymnastic robot, stability analysis of the closed-loop system becomes a very difficult task because of the time-delay dynamics described by a difference-differential equation. A modified delayed feedback control method, called Prediction-based DFC (PDFC), is proposed to stabilize the giant swing motion of two-link horizontal bar gymnastic robot.

2.1. Two-link gymnastic robot model

The two-link horizontal bar gymnastic robot is a simplified model of a human gymnast on a high bar, where the first joint being passive models the gymnast's hands on the bar and the second joint comprising of an actuator models the gymnast's hips. The formula m_i, l_i, a_i, $I_i (i = 1, 2)$ in **Figure 1** denotes the ith link's mass, length, distance from joint to its center of mass, inertia moment around its center of mass, respectively.

http://dx.doi.org/10.5772/65831

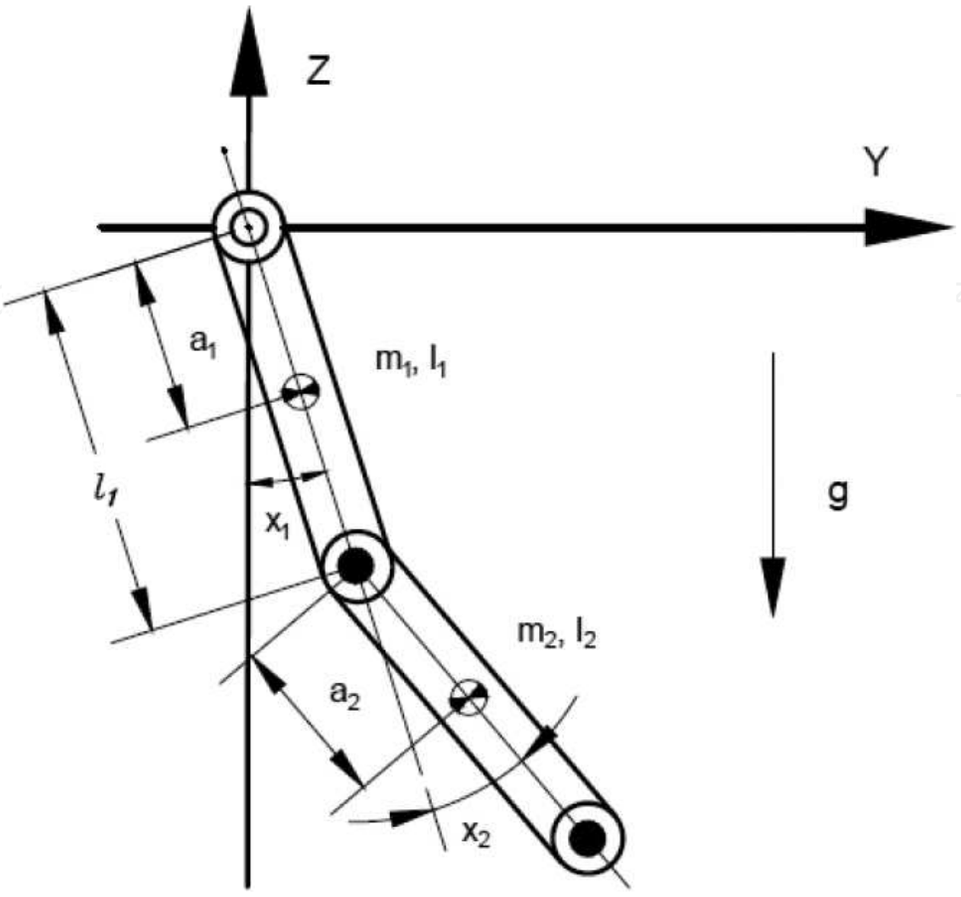

Figure 1. Two-link gymnastic robot model.

The equation of motion of the gymnastic robot is as follows:

$$\begin{bmatrix} u_1 \\ u_2 \end{bmatrix} = \underbrace{\begin{bmatrix} M_{11} & M_{12} \\ M_{21} & M_{22} \end{bmatrix}}_{M} \begin{bmatrix} \ddot{x}_1 \\ \ddot{x}_2 \end{bmatrix} + \underbrace{\begin{bmatrix} C_1 \\ C_2 \end{bmatrix}}_{C} + \underbrace{\begin{bmatrix} G_1 \\ G_2 \end{bmatrix}}_{G}, \tag{1}$$

where $\mathbf{x} = (x_1, x_2)^T \in \mathrm{R}^2$ is the generalized coordinate vector, $\mathbf{u} = (u_1, u_2)^T \in \mathrm{R}^2$ is the joint torque vector, and $M \in \mathrm{R}^{2\times 2}$, $C \in \mathrm{R}^{2\times 1}$, $G \in \mathrm{R}^{2\times 1}$ denote the inertia matrix, Coriolis matrix, and gravitational matrix, respectively.

$$M_{11} = I_1 + I_2 + m_1 a_1^2 + m_2\left(l_1^2 + a_2^2 + 2l_1 a_2 \cos x_2\right)$$

$$M_{12} = I_2 + m_2\left(a_2^2 + l_1 a_2 \cos x_2\right)$$

$$M_{21} = I_2 + m_2\left(a_2^2 + l_1 a_2 \cos x_2\right)$$

$$M_{22} = I_2 + m_2 a_2^2$$

$$C_1 = -\left(\dot{x}_2^2 + 2\dot{x}_1\dot{x}_2\right) m_2 l_1 a_2 \sin x_2$$

$$C_2 = \dot{x}_1^2 m_2 l_1 a_2 \sin x_2$$

$$G_1 = g\{(m_1a_1 + m_2l_1)\sin x_1 + m_2a_2\sin(x_1 + x_2)\}$$

$$G_2 = gm_2a_2\sin(x_1 + x_2)$$

In addition, since the first joint cannot generate active torque, the following constraint must be satisfied.

$$u_1 \equiv h(\ddot{\mathbf{x}}, \dot{\mathbf{x}}, \mathbf{x}) = 0 \tag{2}$$

In order to facilitate the analysis, we rewrite the motion Eq. (1) into the following equation of state:

$$\dot{x} = \begin{bmatrix} \dot{\mathbf{x}} \\ M^{-1}(\mathbf{x})(-C(\mathbf{x}, \dot{\mathbf{x}}) - G(\mathbf{x})) \end{bmatrix} + \begin{bmatrix} 0 \\ M^{-1}(\mathbf{x})E \end{bmatrix} u \equiv f(x, u), \tag{3}$$

where

$$\begin{aligned} M(\mathbf{x}) &= \begin{bmatrix} c_1 + c_2 + 2d\cos x_2 & c_2 + d\cos x_2 \\ c_2 + d\cos x_2 & c_2 \end{bmatrix}, \\ C(\mathbf{x}, \dot{\mathbf{x}}) &= \begin{bmatrix} -(\dot{x}_2^2 + 2\dot{x}_1\dot{x}_2)d\sin x_2 \\ \dot{x}_1^2 d\sin x_2 \end{bmatrix}, \\ G(\mathbf{x}) &= \begin{bmatrix} g_1\sin x_1 + g_2\sin(x_1 + x_2) \\ g_2\sin(x_1 + x_2) \end{bmatrix}, \\ E &= \begin{bmatrix} 0 \\ 1 \end{bmatrix}. \end{aligned} \tag{4}$$

Here, $x = [\mathbf{x}, \dot{\mathbf{x}}]^T \in \mathrm{R}^4$ denotes the state vector, and $u \in \mathrm{R}^1$ represents the control input. Meanwhile, the variables among the above equations are defined as follows:

$$c_1 = I_1 + m_1a_1^2 + m_2l_1^2C$$

$$c_2 = I_2 + m_2a_2^2C$$

$$d = m_2l_1a_2C$$

$$g_1 = g(m_1a_1 + m_2l_1)C$$

$$g_2 = gm_2a_2.$$

2.2. Prediction-based delayed feedback control

As is known, the stability of a periodic orbit of the original continuous-time system is closely related to the stability of the fixed point of the corresponding Poincaré map. Since the stability of the periodic orbit means that the sequence of points converges to a fixed point in the phase plane, the objective system can be expressed as the following difference equation for the discrete-time systems.

http://dx.doi.org/10.5772/65831

$$\tilde{x}(k+1) = A\tilde{x}(k) + Bu(k) \equiv f(\tilde{x}(k), u(k)) \tag{5}$$

where k, $\tilde{x} \in R^4$, $u \in R^1$ denote the discrete time, the state error, and the control input, respectively. And $A \in R^{4 \times 4}$ is named as the error transfer matrix (ETM), $B \in R^{4 \times 1}$ is called the Input Matrix.

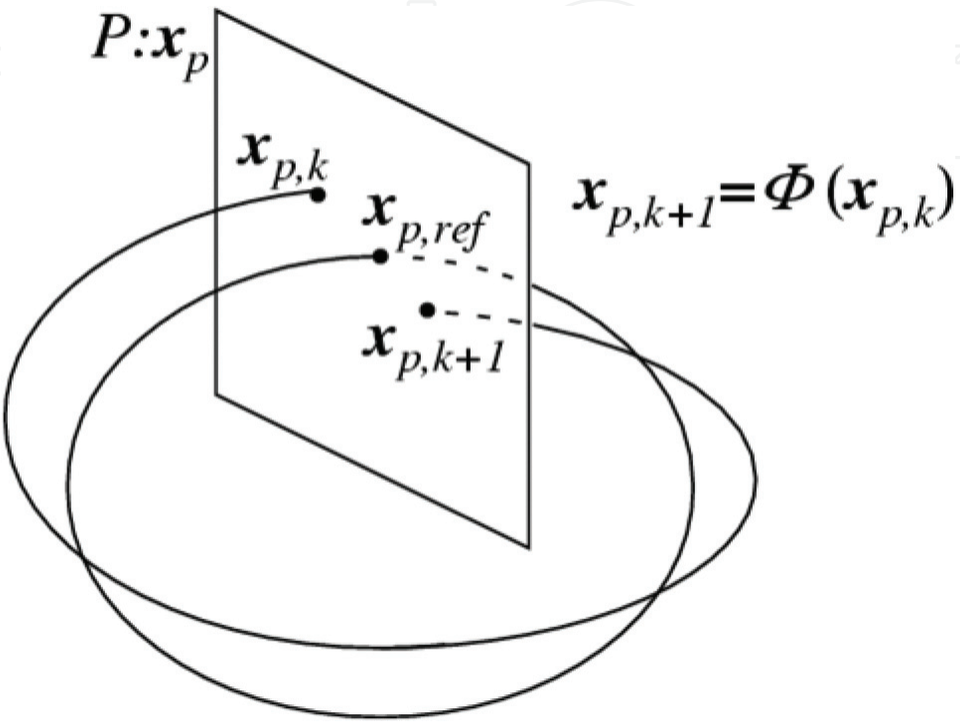

Figure 2. Poincaré map of a closed periodic trajectory.

2.2.1. Solution for obtaining the error transfer matrix **A**

Here, let $y_1 = \dot{x}_1$, $y_2 = \dot{x}_2$. Then the state vector of two-link gymnastic robot can be written in the following form:

$$x = (x_1, x_2, y_1, y_2) \tag{6}$$

As shown in **Figure 2**, the $(k+1)$th state vector $x_{p,k+1}$ can be calculated by one-cycle integration in accordance with the control law by defining the kth state vector passing through the section P as $x_{p,k}$.

This relationship representing this state transfer map is defined as ϕ as follows:

$$x_{p,k+1} = \phi(x_{p,k}) \tag{7}$$

If given an initial condition from which a periodic orbit can be formed, it will return to the same point after one period. Hence, the following equation holds:

$$x_{p,ref} = \phi\left(x_{p,ref}\right) \tag{8}$$

While a difference occurs in the initial state, the motion will stray away from the periodic orbit. Suppose that there was an error corresponding to $e_{p,k}$ in kth state vector, the $(k+1)$th state $x_{p,k+1}$ can be described as

$$x_{p,k+1} = \phi\left(x_{p,ref} + e_{p,k}\right). \tag{9}$$

Using the above equation's Taylor series at $e_{p,k}$ and neglecting the higher-order terms can yield

$$e_{p,k+1} = \frac{\partial\phi\left(x_{p,ref}\right)}{\partial x_p} e_{p,k} \equiv A e_{p,k}. \tag{10}$$

It is obvious that $\partial\phi(x_{p,ref})/\partial x_p$ is equivalent to the ETM A defined in Eq. (5). It can be judged from this equation that if the absolute value of the ETM's eigenvalue >1, then the error increases with each cycle, and if <1, the motion will approach asymptotically the periodic orbit. However, because the state transfer mapping cannot be stated explicitly as a function, in previous studies, this ETM had been computed based on numerical differentiation. In this work, we obtained ETM with an analytical method by using variational equation.

Now consider the objective system given by the equation of motion in Eq. (3). First, given the case of $u = 0$, the objective system becomes

$$\dot{x} = f(x(t)) \equiv \left[f_1, f_2, f_3, f_4\right]^T \tag{11}$$

Assume the state x to be the following vector function

$$x(t) = \varphi(t, x) \equiv \left[\varphi_1, \varphi_2, \varphi_3, \varphi_4\right]^T, \tag{12}$$

where f_i, φ_i ($i = 1 \sim 4$) are the functions of x. The solution of equation passing through $x(0)$ at $t = 0$ is defined as follows:

$$x(0) = x_0. \tag{13}$$

Moreover, the periodic solution satisfies the following equation.

$$x(T) = x(0) = \varphi(T, x_0) \tag{14}$$

Here, a Poincaré map is defined as follows:

$$P: \begin{array}{l} \mathbf{R}^n \to \mathbf{R}^n \quad (n = 4) \\ x_0 \mapsto x_1 = P(x_0) = \varphi(T, x_0) \end{array}$$

Then, the T-period sequence of points obtained by sampling the trajectory from the initial value x_0 is

$$\{x_0, x_1, ., x_k, \ldots\} = \{x_0, P(x_0), P^2(x_0), ., P^k(x_0), \ldots\}. \tag{15}$$

Thus, it is obvious that the periodic solution is shown as a point passing through the same position. Substituting $x = \varphi(t, x_0)$ into Eq. (11), we obtain an equation for the variable $\varphi(t, x_0)$, which can be written as

$$\frac{d\varphi(t, x_0)}{dt} = f(\varphi(t, x_0)). \tag{16}$$

Next, taking differentiation for Eq. (16) at x_0, we can obtain

$$\frac{\partial}{\partial x_0}\left(\frac{d\varphi}{dt}(t, x_0)\right) = \frac{\partial}{\partial x_0}(f(\varphi(t, x_0))). \tag{17}$$

The differential order of the left-hand side in the above equation can be modified as

$$\frac{d}{dt}\left(\frac{\partial\varphi}{\partial x_0}(t, x_0)\right) = \frac{\partial f}{\partial x}(\varphi(t, x_0))\frac{\partial\varphi}{\partial x_0}(t, x_0) \equiv \tilde{A}(t)\frac{\partial\varphi}{\partial x_0}(t, x_0). \tag{18}$$

Thus, it becomes a time-varying linear matrix differential equation with the form of

$$\frac{dX(t, x_0)}{dt} = \tilde{A}(t)X(t, x_0), \tag{19}$$

which is called the Variational Equation if defining $X(t, x_0) = \frac{\partial\varphi}{\partial x_0}(t, x_0)$. From Eqs. (11) and (12), the above equation is equivalent to

$$\frac{d}{dt}\begin{bmatrix} \partial\varphi_1/\partial x_{i,0} \\ \partial\varphi_2/\partial x_{i,0} \\ \partial\varphi_3/\partial x_{i,0} \\ \partial\varphi_4/\partial x_{i,0} \end{bmatrix} = \begin{bmatrix} \partial f_1/\partial x_1 & \partial f_1/\partial x_2 & \partial f_1/\partial y_1 & \partial f_1/\partial y_2 \\ \partial f_2/\partial x_1 & \partial f_2/\partial x_2 & \partial f_2/\partial y_1 & \partial f_2/\partial y_2 \\ \partial f_3/\partial x_1 & \partial f_3/\partial x_2 & \partial f_3/\partial y_1 & \partial f_3/\partial y_2 \\ \partial f_4/\partial x_1 & \partial f_4/\partial x_2 & \partial f_4/\partial y_1 & \partial f_4/\partial y_2 \end{bmatrix} \begin{bmatrix} \partial\varphi_1/\partial x_{i,0} \\ \partial\varphi_2/\partial x_{i,0} \\ \partial\varphi_3/\partial x_{i,0} \\ \partial\varphi_4/\partial x_{i,0} \end{bmatrix}, \tag{20}$$

where $x_{i,0}$ refers to the solution at $t = 0$ of the ith state corresponding to the state vector x defined in Eq. (12).

Note that $X(0, x_0) = I$. Carrying out integrals in numerical integration to the above variational equations over the interval $t \in [0, T]$, one column of the matrix $X(T, x_0)$ can be obtained. Hence, repeating it four times, all of its values can be calculated. It should be emphasized here that to solve these equations since the value of $\tilde{A}(t)$ is required, however, $\tilde{A}(t)$ contains $x(t)$ in terms of the relevant time, they have to be solved together with Eq. (11) simultaneously. From Eqs. (10) and (15), it is not difficult to be verified that $X(T, x_0)$ can be regarded as ETM.

2.2.2. Solution for obtaining the input matrix B

Note that Eq. (3) can be rewritten into

$$\dot{x} = \tilde{f}(x,u) = f(x) + g(x)u, \tag{21}$$

where

$$g(x) = \begin{bmatrix} 0 \\ M^{-1}(x)E \end{bmatrix} \equiv \begin{bmatrix} 0 \\ 0 \\ g_3 \\ g_4 \end{bmatrix}. \tag{22}$$

The input torque u can be described as

$$u = \mathrm{rect}(t)u_0, \tag{23}$$

where

$$\mathrm{rect}(t) = \begin{cases} 1 & \text{if} \quad kT < t \le kT + \tau \quad (k = 0,1,2,\ldots) \\ 0 & \text{otherwise} \end{cases}, \tag{24}$$

Here, u_0 is the control input during (t_0, τ), while $x = x_0$ and τ are control parameters.

Since the solution of equation at $x = x(0)$ can be stated as

$$x(t) = \varphi(t, x_0, u_0). \tag{25}$$

Define a Poincaré map as follows:

$$\tilde{P}: \begin{array}{l} \mathrm{R}^n \to \mathrm{R}^n \quad (n = 4) \\ x_0 \mapsto x_1 = P(x_0, u_0) = \varphi(T, x_0, u_0) \end{array}$$

The continuous system described by Eq. (21) will change to be a discrete system by mapping of $\tilde{P}$. Substituting $x = \varphi(t, x_0, u_0)$ into Eq. (21), the following equation for the variable $\varphi(t, x_0)$ can be obtained.

$$\frac{d\varphi(t, x_0, u_0)}{dt} = f(\varphi(t, x_0, u_0)) + g(x)\,\mathrm{rect}(t)u_0 \tag{26}$$

It is obvious here that by taking differentiation at x_0, its result will be equivalent to Eq. (18). Consider here the case of differentiation at u_0, which can yield

$$\frac{\partial}{\partial u_0}\left(\frac{d\varphi}{dt}(t, x_0, u_0)\right) = \frac{\partial}{\partial u_0}(f(\varphi(t, x_0, u_0))) + g(x)\,\mathrm{rect}(t). \tag{27}$$

The differential order of left-hand side in the above equation can also be changed.

$$\frac{d}{dt}\left(\frac{\partial\varphi}{\partial u_0}(t, x_0, u_0)\right) = \frac{\partial f}{\partial x}(\varphi(t, x_0, u_0))\frac{\partial\varphi}{\partial u_0}(t, x_0, u_0) + g(x)\,\mathrm{rect}(t) \tag{28}$$

Let $X(t, x_0, u_0) = \partial\varphi/\partial x_0(t, x_0, u_0)$. Similar to previous subsection, the above equation is equivalent to the following equation.

http://dx.doi.org/10.5772/65831

$$\frac{d}{dt}\begin{bmatrix}\partial\varphi_1/\partial u_0\\ \partial\varphi_2/\partial u_0\\ \partial\varphi_3/\partial u_0\\ \partial\varphi_4/\partial u_0\end{bmatrix} = \begin{bmatrix}\partial f_1/\partial x_1 & \partial f_1/\partial x_2 & \partial f_1/\partial y_1 & \partial f_1/\partial y_2\\ \partial f_2/\partial x_1 & \partial f_2/\partial x_2 & \partial f_2/\partial y_1 & \partial f_2/\partial y_2\\ \partial f_3/\partial x_1 & \partial f_3/\partial x_2 & \partial f_3/\partial y_1 & \partial f_3/\partial y_2\\ \partial f_4/\partial x_1 & \partial f_4/\partial x_2 & \partial f_4/\partial y_1 & \partial f_4/\partial y_2\end{bmatrix}\begin{bmatrix}\partial\varphi_1/\partial u_0\\ \partial\varphi_2/\partial u_0\\ \partial\varphi_3/\partial u_0\\ \partial\varphi_4/\partial u_0\end{bmatrix} + \operatorname{rect}(t)\begin{bmatrix}0 & 0 & g_3 & g_4\end{bmatrix}^T \tag{29}$$

Note that $X(0, x_0, u_0) = 0$. Carrying out integrals in numerical integration to Eq. (29) over the interval $t \in [0, T]$, it is not difficult to obtain the value of the matrix $X(T, x_0, u_0)$ which can be regarded as the input matrix B defined in Eq. (5).

2.2.3. Stability of periodic orbits

Since the value of both the matrices A and B can be calculated analytically, i.e., the continuous system of two-link gymnastic robot can be expressed in a discrete model described in Eq. (5). In order to study the stabilization of gymnastic robot's continuous system by delayed feedback control, it is sufficient to consider the discrete model.

Consider the following Prediction-based feedback control:

$$u(k) = K\{x(k) - x_P(k)\}, \tag{30}$$

where $K \in \mathrm{R}^{1\times 4}$ is a feedback gain, $x(k)$ is the state vector at k-step, $x_P(k)$ denotes one period future states of uncontrolled system which can be obtained from Eq. (3). Moreover, notice that the following almost equality holds.

$$x(k) - x_P(k) \approx \tilde{x}(k) - f(\tilde{x}(k), 0) \tag{31}$$

Here $f(\tilde{x}(k), 0)$ stands for the state error at $(k + 1)$th step. From Eq. (5), it is obvious that $f(\tilde{x}(k), 0) = A\tilde{x}(k)$ holds.

Therefore, the closed-loop system can be described by

$$\begin{aligned}\tilde{x}(k+1) &= A\tilde{x}(k) + BK(I-A)\tilde{x}(k)\\ &= \{A + BK(I-A)\}\tilde{x}(k).\end{aligned} \tag{32}$$

Let

$$\widehat{K} = K(I-A), \tag{33}$$

then the stabilization problem is reduced as follows:

Given a system Eq. (5), find a feedback gain $\widehat{K}$ that places the closed-loop poles of the system in the set

$$\Lambda = \{z \in \mathbf{C} : |z| < 1\}. \tag{34}$$

By using the pole placement technique, it is not difficult to obtain the value of $\widehat{K}$, and if $det\ (I - A) \neq 0$, then the feedback gain K is given by

$$K = \widehat{K}(I - A)^{-1}. \tag{35}$$

Thus, the above design procedure can be applied to analyze the stability of two-link gymnastic robot system.

3. Delayed feedback control for a four-link horizontal bar gymnastic robot

As is known, the simplified two-link robot shown in the previous section is not an ideal physical model of a human gymnast on a high bar. In order to mimic gymnastic routine more realistically, the complicated robot model with higher degrees of freedom (DOF) needs to be considered. An improved method based on PDFC which control a three-link gymnastic robot via a periodic gain has been proposed [51]. In this section, the Multiprediction Delayed Feedback Control (MDFC), is extended to a more complicated gymnastic robot with four DOF.

3.1. Four-link gymnastic robot model

Figure 3 shows a four-link horizontal bar gymnastic robot model, which consists of four links and four joints. Shoulder, hips, and knees are active, while the pivot connecting the hand and bar is a passive joint. Assume m_i, l_i, a_i, $I_i (i = 1, 2, 3, 4)$ to be the link mass, length, distance from joint to its center of mass, and inertia moment around its center of mass, respectively.

The motion equation of the robot is

$$\begin{bmatrix} u_1 \\ u_2 \\ u_3 \\ u_4 \end{bmatrix} = \begin{bmatrix} M_{11} & M_{12} & M_{13} & M_{14} \\ M_{21} & M_{22} & M_{23} & M_{24} \\ M_{31} & M_{32} & M_{33} & M_{34} \\ M_{41} & M_{42} & M_{43} & M_{44} \end{bmatrix} \begin{bmatrix} \ddot{x}_1 \\ \ddot{x}_2 \\ \ddot{x}_3 \\ \ddot{x}_4 \end{bmatrix} + \begin{bmatrix} C_1 \\ C_2 \\ C_3 \\ C_4 \end{bmatrix} + \begin{bmatrix} G_1 \\ G_2 \\ G_3 \\ G_4 \end{bmatrix}, \tag{36}$$

where $\mathbf{x} = (x_1, x_2, x_3, x_4)^T \in \mathrm{R}^4$ is the generalized coordinate vector, $(u_1, u_2, u_3, u_4)^T \in \mathrm{R}^4$ is the joint torque vector, and M_{ij}, C_i, G_i $(i, j = 1, 2, 3, 4)$ are, respectively, the terms of inertia matrix, Coriolis matrix, and gravitational matrix. Each item of M_{ij}, C_i, G_i is as follows. Note that $M_{ij} = M_{ji}$, $(i \neq j)$.

$$\begin{aligned} \mathrm{M11} = {} & m_2\left(2a_2l_1\cos(x_2) + a_2^2 + l_1^2\right) + m_3\{2a_3l_1\cos(x_2 + x_3) + 2a_3l_2\cos(x_3) \\ & + a_3^2 + 2l_1l_2\cos(x_2) + l_1^2 + l_2^2\} + m_4\{2a_4l_1\cos(x_2 + x_3 + x_4) + 2a_4l_2\cos(x_3 + x_4) \\ & + 2a_4l_3\cos(x_4) + a_4^2 + 2l_1l_2\cos(x_2) + 2l_1l_3\cos(x_2 + x_3) + 2l_2l_3\cos(x_3) + l_1^2 + l_2^2 + l_3^2\} \\ & + a_1^2m_1 + I_1 + I_2 + I_3 + I_4; \end{aligned}$$

$$\begin{aligned} \mathrm{M12} = {} & m_2\left(a_2l_1\cos(x_2) + a_2^2\right) + m_3\left\{a_3l_1\cos(x_2 + x_3) + 2a_3l_2\cos(x_3) + a_3^2 + l_1l_2\cos(x_2) + l_2^2\right\} \\ & + m_4\left\{a_4l_1\cos(x_2 + x_3 + x_4) + 2a_4l_2\cos(x_3 + x_4) + 2a_4l_3\cos(x_4) + a_4^2 + l_1l_2\cos(x_2)\right. \\ & \left. + l_1l_3\cos(x_2 + x_3) + 2l_2l_3\cos(x_3) + l_2^2 + l_3^2\right\} + I_2 + I_3 + I_4; \end{aligned}$$

http://dx.doi.org/10.5772/65831

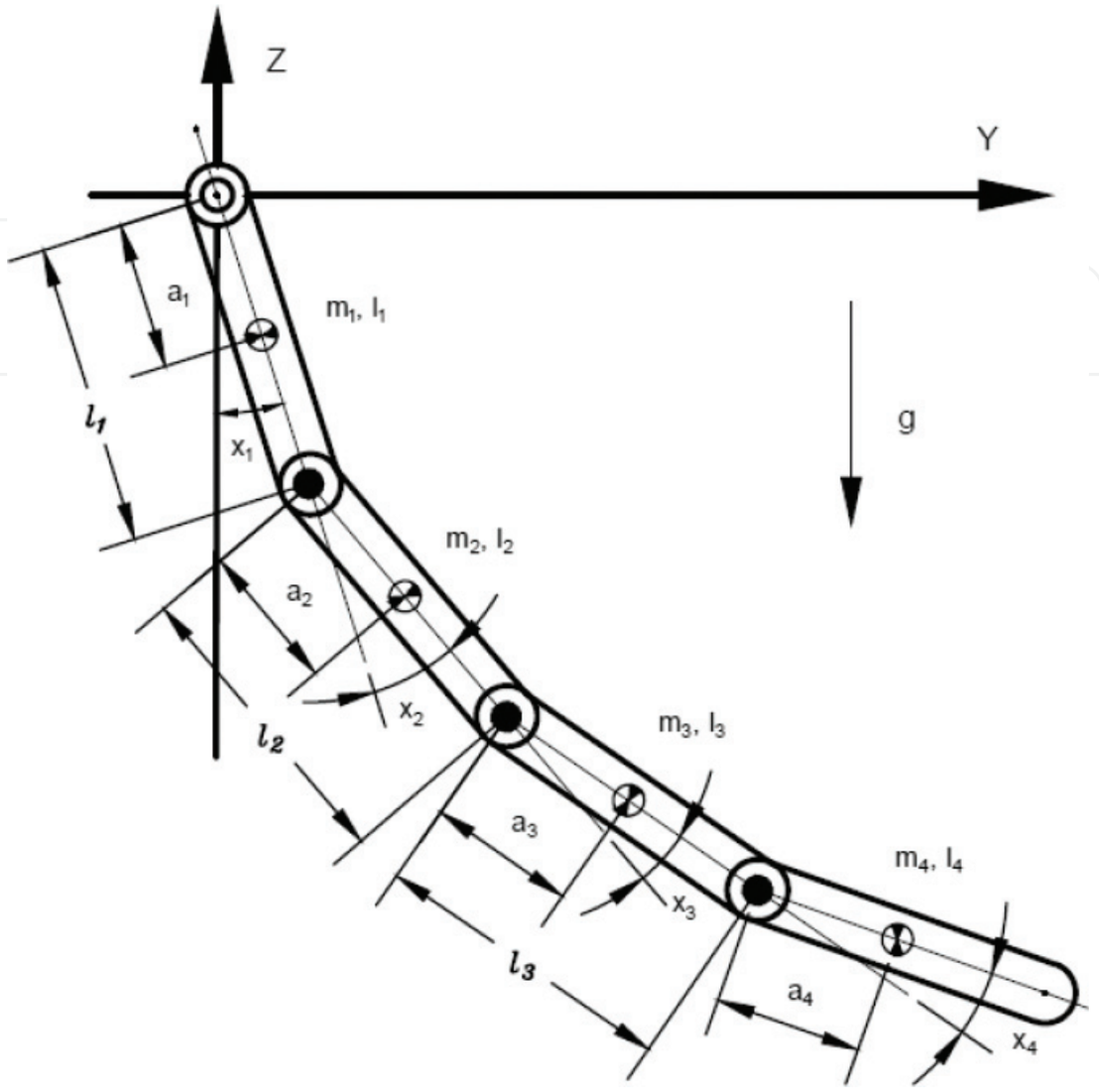

Figure 3. Four-link gymnastic robot model.

$$\mathrm{M13} = m_3\left(a_3 l_1 \cos\left(x_2 + x_3\right) + a_3 l_2 \cos\left(x_3\right) + a_3^2\right) + m_4\{a_4 l_1 \cos\left(x_2 + x_3 + x_4\right) + a_4 l_2 \cos\left(x_3 + x_4\right)$$
$$+2a_4 l_3 \cos\left(x_4\right) + a_4^2 + l_1 l_3 \cos\left(x_2 + x_3\right) + l_3\left(l_2 \cos\left(x_3\right) + l_3\right)\} + I_3 + I_4;$$

$$\mathrm{M14} = m_4\left(a_4 l_1 \cos\left(x_2 + x_3 + x_4\right) + a_4 l_2 \cos\left(x_3 + x_4\right) + a_4 l_3 \cos\left(x_4\right) + a_4^2\right) + I_4;$$

$$\mathrm{M22} = m_3\left(2a_3 l_2 \cos\left(x_3\right) + a_3^2 + l_2^2\right) + m_4\left\{2a_4 l_2 \cos\left(x_3 + x_4\right) + 2a_4 l_3 \cos\left(x_4\right) + a_4^2\right.$$
$$\left.+2l_2 l_3 \cos\left(x_3\right) + l_2^2 + l_3^2\right\} + a_2^2 m_2 + I_2 + I_3 + I_4;$$

$$\mathrm{M23} = m_3\left(a_3 l_2 \cos\left(x_3\right) + a_3^2\right) + m_4\left\{a_4 l_2 \cos\left(x_3 + x_4\right) + 2a_4 l_3 \cos\left(x_4\right) + a_4^2\right.$$
$$\left.+l_2 l_3 \cos\left(x_3\right) + l_3^2\right\} + I_3 + I_4;$$

$$\mathrm{M24} = m_4\left(a_4 l_2 \cos\left(x_3 + x_4\right) + a_4 l_3 \cos\left(x_4\right) + a_4^2\right) + I_4;$$

$$\mathrm{M33} = m_4\left(2a_4l_3\cos\left(x_4\right) + a_4^2 + l_3^2\right) + a_3^2m_3 + I_3 + I_4;$$

$$\mathrm{M34} = m_4\left(a_4l_3\cos\left(x_4\right) + a_4^2\right) + I_4;$$

$$\mathrm{M44} = a_4^2m_4 + I_4;$$

$$\mathrm{C1} = m_3\{-a_3l_2\dot{q}_3\left(2\left(\dot{q}_1 + \dot{q}_2\right) + \dot{q}_3\right)\sin\left(x_3\right) - a_3l_1\left(\dot{q}_2 + \dot{q}_3\right)\left(2\dot{q}_1 + \dot{q}_2 + \dot{q}_3\right)$$
$$\sin\left(x_2 + x_3\right) - l_1l_2\dot{q}_2\left(2\dot{q}_1 + \dot{q}_2\right)\sin\left(x_2\right)\} - a_2l_1m_2\dot{q}_2\left(2\dot{q}_1 + \dot{q}_2\right)\sin\left(x_2\right)$$
$$+ m_4\{-a_4l_3\dot{q}_4\left(2\left(\dot{q}_1 + \dot{q}_2 + \dot{q}_3\right) + \dot{q}_4\right)\sin\left(x_4\right) - a_4l_2\left(\dot{q}_3 + \dot{q}_4\right)\left(2\dot{q}_1 + 2\dot{q}_2 + \dot{q}_3 + \dot{q}_4\right)$$
$$\sin\left(x_3 + x_4\right) - a_4l_1\left(\dot{q}_2 + \dot{q}_3 + \dot{q}_4\right)\left(2\dot{q}_1 + \dot{q}_2 + \dot{q}_3 + \dot{q}_4\right)\sin\left(x_2 + x_3 + x_4\right)$$
$$+ l_2l_3\dot{q}_3^2(-\sin\left(x_3\right)) - 2l_2l_3\left(\dot{q}_1 + \dot{q}_2\right)\dot{q}_3\sin\left(x_3\right) + l_2l_3\dot{q}_3^2(-\sin\left(x_3\right)) - 2l_2l_3\left(\dot{q}_1 + \dot{q}_2\right)\dot{q}_3\sin\left(x_3\right)$$

$$\mathrm{C2} = a_2l_1m_2\dot{q}_1^2\sin\left(x_2\right) + m_3\{a_3l_1\dot{q}_1^2\sin\left(x_2 + x_3\right) - 2a_3l_2\dot{q}_3\dot{q}_1\sin\left(x_3\right) - a_3l_2\dot{q}_3^2\sin\left(x_3\right)$$
$$-2a_3l_2\dot{q}_2\dot{q}_3\sin\left(x_3\right) + l_1l_2\dot{q}_1^2\sin\left(x_2\right)\} + m_4\{a_4l_1\dot{q}_1^2\sin\left(x_2 + x_3 + x_4\right)$$
$$-2a_4l_3\dot{q}_4\dot{q}_1\sin\left(x_4\right) - 2a_4l_2\dot{q}_3\dot{q}_1\sin\left(x_3 + x_4\right) - 2a_4l_2\dot{q}_4\dot{q}_1\sin\left(x_3 + x_4\right) - a_4l_3\dot{q}_4^2\sin\left(x_4\right)$$
$$-2a_4l_3\dot{q}_2\dot{q}_4\sin\left(x_4\right) - 2a_4l_3\dot{q}_3\dot{q}_4\sin\left(x_4\right) - a_4l_2\dot{q}_3^2\sin\left(x_3 + x_4\right) - a_4l_2\dot{q}_4^2\sin\left(x_3 + x_4\right)$$
$$-2a_4l_2\dot{q}_2\dot{q}_3\sin\left(x_3 + x_4\right) - 2a_4l_2\dot{q}_2\dot{q}_4\sin\left(x_3 + x_4\right) - 2a_4l_2\dot{q}_3\dot{q}_4\sin\left(x_3 + x_4\right) + l_1l_2\dot{q}_1^2\sin\left(x_2\right)$$
$$+ l_1l_3\dot{q}_1^2\sin\left(x_2 + x_3\right) - 2l_2l_3\dot{q}_3\dot{q}_1\sin\left(x_3\right) - l_2l_3\dot{q}_3^2\sin\left(x_3\right) - 2l_2l_3\dot{q}_2\dot{q}_3\sin\left(x_3\right)\};$$

$$\mathrm{C3} = m_3\left\{a_3l_1\dot{q}_1^2\sin\left(x_2 + x_3\right) + a_3l_2\left(\dot{q}_1 + \dot{q}_2\right)^2\sin\left(x_3\right)\right\} + m_4\{a_4l_1\dot{q}_1^2\sin\left(x_2 + x_3 + x_4\right)$$
$$-2a_4l_3\dot{q}_4\dot{q}_1\sin\left(x_4\right) + a_4l_2\left(\dot{q}_1 + \dot{q}_2\right)^2\sin\left(x_3 + x_4\right) - a_4l_3\dot{q}_4^2\sin\left(x_4\right) - 2a_4l_3\dot{q}_2\dot{q}_4\sin\left(x_4\right)$$
$$-2a_4l_3\dot{q}_3\dot{q}_4\sin\left(x_4\right) + l_1l_3\dot{q}_1^2\sin\left(x_2 + x_3\right) + l_2l_3\dot{q}_1^2\sin\left(x_3\right) + 2l_2l_3\dot{q}_2\dot{q}_1\sin\left(x_3\right) + l_2l_3\dot{q}_2^2\sin\left(x_3\right)\};$$

$$\mathrm{C4} = m_4\{a_4l_1\dot{q}_1^2\sin\left(x_2 + x_3 + x_4\right) + a_4l_3\dot{q}_1^2\sin\left(x_4\right) + 2a_4l_3\dot{q}_2\dot{q}_1\sin\left(x_4\right) + 2a_4l_3\dot{q}_3\dot{q}_1\sin\left(x_4\right)$$
$$+ a_4l_3\dot{q}_2^2\sin\left(x_4\right) + a_4l_2\left(\dot{q}_1 + \dot{q}_2\right)^2\sin\left(x_3 + x_4\right) + a_4l_3\dot{q}_3^2\sin\left(x_4\right) + 2a_4l_3\dot{q}_2\dot{q}_3\sin\left(x_4\right)\};$$

$$\mathrm{G1} = g\{m_2(a_2\sin\left(x_1 + x_2\right) + l_1\sin\left(x_1\right)) + m_3(a_3\sin\left(x_1 + x_2 + x_3\right) + l_1\sin\left(x_1\right)$$
$$+ l_2\sin\left(x_1 + x_2\right)) + m_3(a_3\sin\left(x_1 + x_2 + x_3\right) + l_1\sin\left(x_1\right) + l_2\sin\left(x_1 + x_2\right))$$
$$+ l_2\sin\left(x_1 + x_2\right) + l_3\sin\left(x_1 + x_2 + x_3\right)) + a_1m_1\sin\left(x_1\right)\};$$

$$\mathrm{G2} = g\{m_3(a_3\sin\left(x_1 + x_2 + x_3\right) + l_2\sin\left(x_1 + x_2\right)) + m_4(a_4\sin\left(x_1 + x_2 + x_3 + x_4\right)$$
$$+ l_2\sin\left(x_1 + x_2\right) + l_3\sin\left(x_1 + x_2 + x_3\right)) + a_2m_2\sin\left(x_1 + x_2\right)\};$$

http://dx.doi.org/10.5772/65831

$$\mathrm{G3} = g\{m_4(a_4 \sin(x_1 + x_2 + x_3 + x_4) + l_3 \sin(x_1 + x_2 + x_3)) + a_3 m_3 \sin(x_1 + x_2 + x_3)\};$$

$$\mathrm{G4} = a_4 g m_4 \sin(x_1 + x_2 + x_3 + x_4);$$

Similar to the motion equation of the two-link robot, Eq. (36) can be rewritten as follows.

$$\dot{x} = \begin{bmatrix} y \\ -M^{-1}(x)(C(x) + G(x)) \end{bmatrix} + \begin{bmatrix} 0 \\ M^{-1}(x)E \end{bmatrix} \begin{bmatrix} u_2 \\ u_3 \\ u_4 \end{bmatrix} \equiv f(x, u). \tag{37}$$

3.2. Multiprediction delayed feedback control

As is discussed in the reference [51], multiprediction delayed feedback control is based on a new discretization method to increase the control performance by introducing a notion of plural Poincaré maps, (P_i, P_2,..., P_N) which divide the first link angle $x_1 \in (-\pi, \pi)$ into N sections as shown in **Figure 4**.

By the ith (i = 1, 2,..., N) Poincaré map, the four-link horizontal bar gymnastic robot system can be discretized into the following

$$x(k+1, i) = A_i x(k, i) + B_i u(k, i), \tag{38}$$

where k is the discrete time and $x(k, i)(i = 1, 2,..., N) \in \mathrm{R}^n$, $A_i \in \mathrm{R}^{n \times n}(n = 8)$, $B_i \in \mathrm{R}^{n \times 3}$ denote, respectively, the state error, the error transfer matrix, and the input matrix in terms with the ith Poincaré map. Furthermore, $u(k, i)$ is defined as

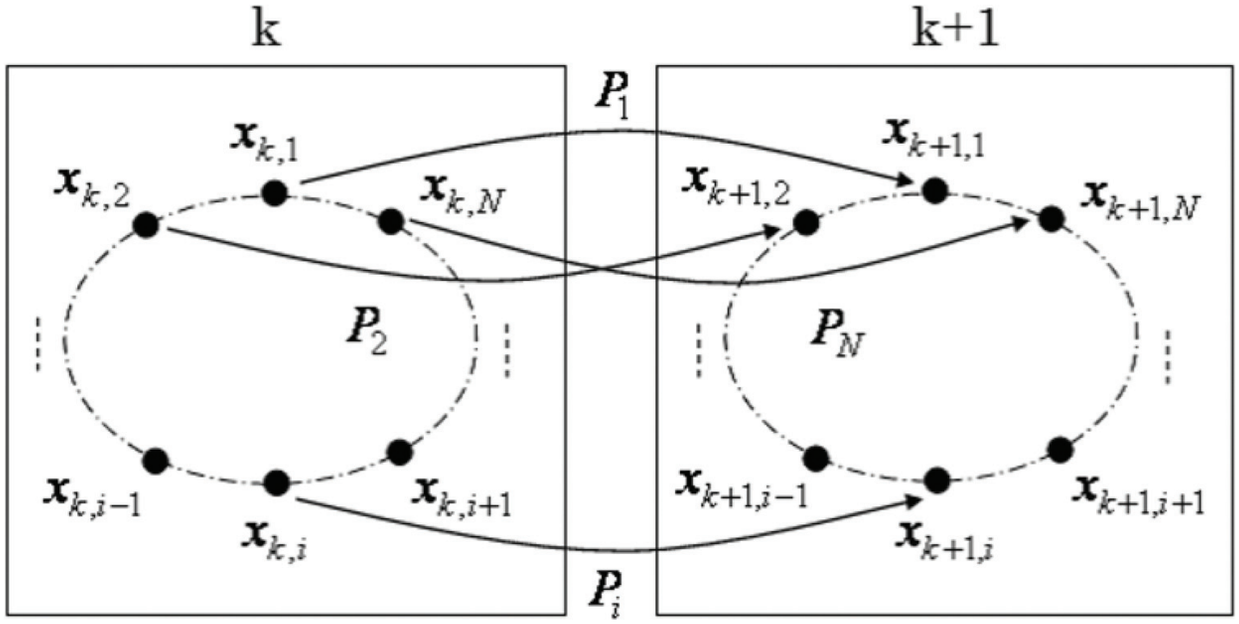

Figure 4. Image of Poincaré maps [51].

$$u(k,i) = K_i\{x(k,i) - x(k+1,i)\} = \widehat{K}_i x(k,i). \tag{39}$$

Here, the equivalence of $\widehat{K}_i \equiv K_i(I - A_i)$ and $K_i = K_{i+N} \in \mathrm{R}^{3\times n}$ are satisfied for each i. By introducing the variable of control period, τ, and defining u_0 as the control input to the system during (t_0, τ) while $x = x_0$, the input torque u is described as

$$u = \mathrm{rect}\,(t)u_0, \tag{40}$$

where rect(t) is a rectangular function as Eq. (41).

$$\mathrm{rect}\,(t) = \begin{cases} 1 & \text{if} \quad (kT + t_i) < t \le (kT + t_i + \tau) \quad (k = 0, 1, 2, \ldots) \\ 0 & \text{otherwise} \end{cases} \tag{41}$$

Here, t_i is the time at ith Poincaré map $P_i(i = 1, 2, \ldots, N)$.

Summarize the state variables at each one of the ith Poincaré section into one vector as follows:

$$X(k,i) = [x(k,i), \ldots, x(k,N), x(k+1,1), \ldots, x(k+1,i-1)]^T \in \mathrm{R}^{nN} \tag{42}$$

Therefore, the close-loop system relating to X(k, i) can be stated as the following discrete-time system with periodic N.

$$X(k,i+1) = F(i)X(k,i), \tag{43}$$

where,

$$F(i) = \begin{bmatrix} 0 & I & \ldots & 0 & 0 \\ \vdots & \vdots & \ddots & \vdots & \vdots \\ 0 & 0 & \ldots & 0 & I \\ A_i + B_i K_i & 0 & \ldots & 0 & 0 \end{bmatrix}. \tag{44}$$

As it is known, the local stability of such a system can be determined by the eigenvalue of the monodromy matrix as follows:

$$\Phi_F(i+N,i) \equiv F(i+N-1)\cdots F(i+1)F(i). \tag{45}$$

The solution of the error transfer matrix A_i and the input matrix B_i is similar to the determination of the two-link gymnastic robot, so only the difference is shown below.

3.3. Solution for obtaining the error transfer matrix A_i

Here, let $y_1 = \dot{x}_1$, $y_2 = \dot{x}_2$, $y_3 = \dot{x}_3$, $y_4 = \dot{x}_4$. Then the state vector of four-link gymnastic robot becomes

http://dx.doi.org/10.5772/65831

$$x = (x_1, x_2, x_3, x_4, y_1, y_2, y_3, y_4). \tag{46}$$

Consider the objective system given by the equation of motion in Eq. (37). First, given the case of $u = 0$, the objective system becomes

$$\dot{x} = f(x(t)) \equiv [f_1, f_2, f_3, f_4, f_5, f_6, f_7, f_8]^T \tag{47}$$

Assume the state x to be the following vector function

$$x(t) = \varphi(t, x) \equiv [\varphi_1, \varphi_2, \varphi_3, \varphi_4, \varphi_5, \varphi_6, \varphi_7, \varphi_8]^T. \tag{48}$$

where $f_{\tilde{i}}$, $\varphi_{\tilde{i}}(\tilde{i} = 1 \sim 8)$ are the functions of x. Introducing the following definition,

$$\begin{aligned} \varphi^m_{x_{\tilde{i},0}} &= \frac{\partial \varphi_m}{\partial x_{\tilde{i},0}} \quad (\tilde{i} = 1{\sim}8), \\ f^m_{x_j} = \frac{\partial f_m}{\partial x_j}, \quad f^m_{y_j} &= \frac{\partial f_m}{\partial y_j} \quad (m = 1{\sim}8, j = 1{\sim}4) \end{aligned} \tag{49}$$

the variational equation becomes

$$\frac{d}{dt}\begin{bmatrix} \varphi^1_{x_{\tilde{i},0}} \\ \varphi^2_{x_{\tilde{i},0}} \\ \varphi^3_{x_{\tilde{i},0}} \\ \varphi^4_{x_{\tilde{i},0}} \\ \varphi^5_{x_{\tilde{i},0}} \\ \varphi^6_{x_{\tilde{i},0}} \\ \varphi^7_{x_{\tilde{i},0}} \\ \varphi^8_{x_{\tilde{i},0}} \end{bmatrix} = \begin{bmatrix} f^1_{x_1} & f^1_{x_2} & f^1_{x_3} & f^1_{x_4} & f^1_{y_1} & f^1_{y_2} & f^1_{y_3} & f^1_{y_4} \\ f^2_{x_1} & f^2_{x_2} & f^2_{x_3} & f^2_{x_4} & f^2_{y_1} & f^2_{y_2} & f^2_{y_3} & f^2_{y_4} \\ f^3_{x_1} & f^3_{x_2} & f^3_{x_3} & f^3_{x_4} & f^3_{y_1} & f^3_{y_2} & f^3_{y_3} & f^3_{y_4} \\ f^4_{x_1} & f^4_{x_2} & f^4_{x_3} & f^4_{x_4} & f^4_{y_1} & f^4_{y_2} & f^4_{y_3} & f^4_{y_4} \\ f^5_{x_1} & f^5_{x_2} & f^5_{x_3} & f^5_{x_4} & f^5_{y_1} & f^5_{y_2} & f^5_{y_3} & f^5_{y_4} \\ f^6_{x_1} & f^6_{x_2} & f^6_{x_3} & f^6_{x_4} & f^6_{y_1} & f^6_{y_2} & f^6_{y_3} & f^6_{y_4} \\ f^7_{x_1} & f^7_{x_2} & f^7_{x_3} & f^7_{x_4} & f^7_{y_1} & f^7_{y_2} & f^7_{y_3} & f^7_{y_4} \\ f^8_{x_1} & f^8_{x_2} & f^8_{x_3} & f^8_{x_4} & f^8_{y_1} & f^8_{y_2} & f^8_{y_3} & f^8_{y_4} \end{bmatrix} \begin{bmatrix} \varphi^1_{x_{\tilde{i},0}} \\ \varphi^2_{x_{\tilde{i},0}} \\ \varphi^3_{x_{\tilde{i},0}} \\ \varphi^4_{x_{\tilde{i},0}} \\ \varphi^5_{x_{\tilde{i},0}} \\ \varphi^6_{x_{\tilde{i},0}} \\ \varphi^7_{x_{\tilde{i},0}} \\ \varphi^8_{x_{\tilde{i},0}} \end{bmatrix}, \tag{50}$$

where $x_{\tilde{i},0}$ refers to the solution at $t = 0$ of the $\tilde{i}$th state corresponding to the state vector x defined in Eq. (48).

Note that the following equation holds.

$$\begin{aligned} A &= [a_1 \quad a_2 \quad a_3 \quad a_4 \quad a_5 \quad a_6 \quad a_7 \quad a_8] \\ a\tilde{i} &= \left[\varphi^1_{x_{\tilde{i},0}}, \quad \varphi^2_{x_{\tilde{i},0}}, \quad \varphi^3_{x_{\tilde{i},0}}, \quad \varphi^4_{x_{i,0}}, \quad \varphi^5_{x_{\tilde{i},0}}, \quad \varphi^6_{x_{\tilde{i},0}}, \quad \varphi^7_{x_{\tilde{i},0}}, \quad \varphi^8_{x_{\tilde{i},0}}\right]^T (\tilde{i} = 1{\sim}8)., \end{aligned} \tag{51}$$

Carrying out integrals in numerical integration to the variational equations of Eq. (50) over the interval $t \in [0, T]$ by eight times, each item of the error transfer matrix, $A_i(i = 1, 2, \ldots, N)$, can be calculated.

3.4. Solution for obtaining the input matrix B_i

Note that Eq. (37) can be rewritten as

$$\dot{x} = \tilde{f}(x,u) = f(x) + g(x)u. \tag{52}$$

Here,

$$g(x) = \begin{bmatrix} 0_{4\times 3} \\ M^{-1}(x)E \end{bmatrix} \equiv \begin{bmatrix} 0 & 0 & 0 \\ 0 & 0 & 0 \\ 0 & 0 & 0 \\ 0 & 0 & 0 \\ g_{12} & g_{13} & g_{14} \\ g_{22} & g_{23} & g_{24} \\ g_{32} & g_{33} & g_{34} \\ g_{42} & g_{43} & g_{44} \end{bmatrix}. \tag{53}$$

Since the solution of equation at $x = x(0)$ can be written as

$$x(t) = \varphi(t, x_0, u_0). \tag{54}$$

The continuous system described by Eq. (53) will change to be a discrete system by mapping of $\tilde{P}_i$. Substituting Eq. (54) into Eq. (53), the following equation for the variable $\varphi(t, x_0)$ can be obtained.

$$\frac{d\varphi(t,x_0,u_0)}{dt} = f(\varphi(t,x_0,u_0)) + g(x)\,\mathrm{rect}\,(t)u_0 \tag{55}$$

Here, consider the case of differentiation at u_0, which can yield

$$\frac{\partial}{\partial u_0}\left(\frac{d\varphi}{dt}(t,x_0,u_0)\right) = \frac{\partial}{\partial u_0}(f(\varphi(t,x_0,u_0))) + g(x)\,\mathrm{rect}\,(t). \tag{56}$$

Let

$$\varphi^m_{u_{j,0}} = \frac{\partial \varphi_m}{\partial u_{j,0}} \quad (m = 1\sim 8, j = 2,3,4). \tag{57}$$

Similar to previous subsection, Eq. (53) is equivalent to the following equation.

$$\frac{d}{dt}\begin{bmatrix} \varphi^1_{u_{j,0}} \\ \varphi^2_{u_{j,0}} \\ \varphi^3_{u_{j,0}} \\ \varphi^4_{u_{j,0}} \\ \varphi^5_{u_{j,0}} \\ \varphi^6_{u_{j,0}} \\ \varphi^7_{u_{j,0}} \\ \varphi^8_{u_{j,0}} \end{bmatrix} = \begin{bmatrix} f^1_{x_1} & f^1_{x_2} & f^1_{x_3} & f^1_{x_4} & f^1_{y_1} & f^1_{y_2} & f^1_{y_3} & f^1_{y_4} \\ f^2_{x_1} & f^2_{x_2} & f^2_{x_3} & f^2_{x_4} & f^2_{y_1} & f^2_{y_2} & f^2_{y_3} & f^2_{y_4} \\ f^3_{x_1} & f^3_{x_2} & f^3_{x_3} & f^3_{x_4} & f^3_{y_1} & f^3_{y_2} & f^3_{y_3} & f^3_{y_4} \\ f^4_{x_1} & f^4_{x_2} & f^4_{x_3} & f^4_{x_4} & f^4_{y_1} & f^4_{y_2} & f^4_{y_3} & f^4_{y_4} \\ f^5_{x_1} & f^5_{x_2} & f^5_{x_3} & f^5_{x_4} & f^5_{y_1} & f^5_{y_2} & f^5_{y_3} & f^5_{y_4} \\ f^6_{x_1} & f^6_{x_2} & f^6_{x_3} & f^6_{x_4} & f^6_{y_1} & f^6_{y_2} & f^6_{y_3} & f^6_{y_4} \\ f^7_{x_1} & f^7_{x_2} & f^7_{x_3} & f^7_{x_4} & f^7_{y_1} & f^7_{y_2} & f^7_{y_3} & f^7_{y_4} \\ f^8_{x_1} & f^8_{x_2} & f^8_{x_3} & f^8_{x_4} & f^8_{y_1} & f^8_{y_2} & f^8_{y_3} & f^8_{y_4} \end{bmatrix} \begin{bmatrix} \varphi^1_{u_{j,0}} \\ \varphi^2_{u_{j,0}} \\ \varphi^3_{u_{j,0}} \\ \varphi^4_{u_{j,0}} \\ \varphi^5_{u_{j,0}} \\ \varphi^6_{u_{j,0}} \\ \varphi^7_{u_{j,0}} \\ \varphi^8_{u_{j,0}} \end{bmatrix} + \mathrm{rect}\,(t) \times \begin{bmatrix} 0 & 0 & 0 & 0 & g_{1j} & g_{2j} & g_{3j} & g_{4j} \end{bmatrix}^T \tag{58}$$

Note that the following equation holds.

http://dx.doi.org/10.5772/65831

$$B = [b_1 \quad b_2 \quad b_3],$$
$$b_{\tilde{i}} = \left[\varphi^1_{u_{j,0}}, \quad \varphi^2_{u_{j,0}}, \quad \varphi^3_{u_{j,0}}, \quad \varphi^4_{u_{j,0}}, \quad \varphi^5_{u_{j,0}}, \quad \varphi^6_{u_{j,0}}, \quad \varphi^7_{u_{j,0}}, \quad \varphi^8_{u_{j,0}}\right]^T (\tilde{i} = 1,2,3). \tag{59}$$

Carrying out integrals in numerical integration to Eq. (58) over the interval $t \in [0, T]$ by three times, it is not difficult to obtain the value of the input matrix $B_i (i = 1, 2,..., N)$.

4. Numerical simulations

This section shows some simulation results to verify the validity of the proposed prediction-based delayed feedback control for a two-link horizontal bar gymnastic robot. The parameters of the robot model are shown in **Table 1**. The stability of giant swing motion with period $T = 0.7$(s) was examined.

		1st link	2nd link
Mass	m_i (kg)	39.5	20.7
Moment of inertia	I_i (kgm^2)	3.25	1.56
Link length	l_i (m)	1.2	0.879
Offset of mass center	a_i (m)	0.756	0.377

Table 1. Link parameter values.

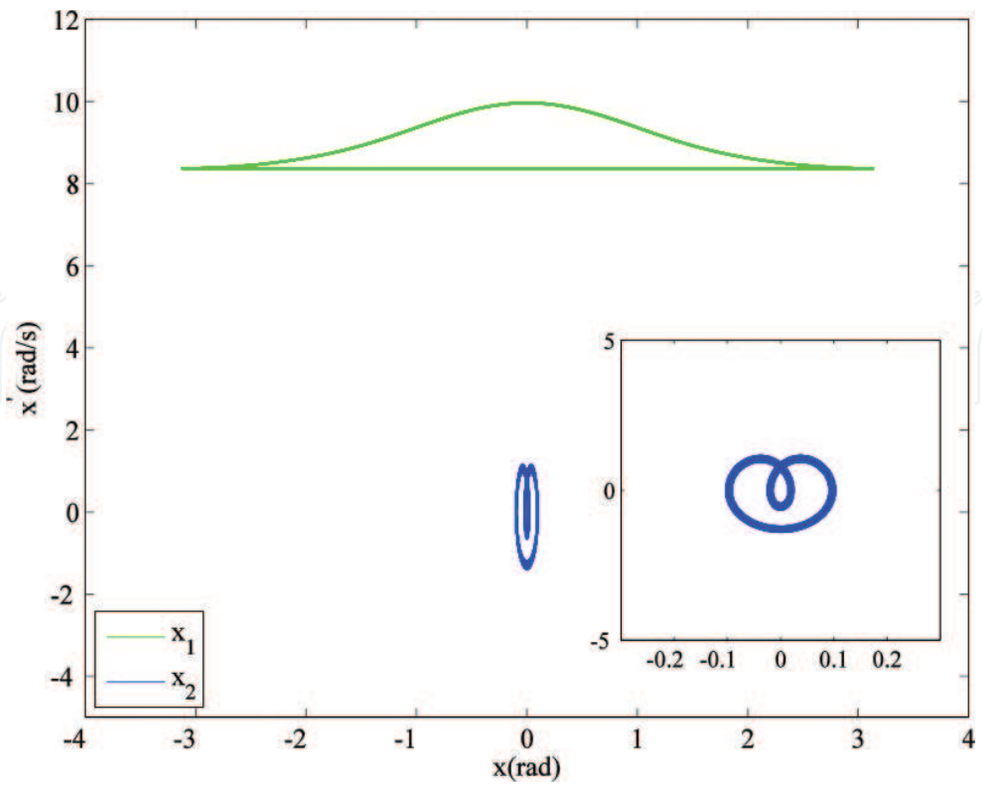

Figure 5. Phase portrait of X–$\dot{x}$ (no error).

By means of the shooting method, an initial condition was obtained such as $x(0) = (\pi, 0.0, 8.352, -1.19)$ that can achieve a free giant swing motion with a period of 0.7(s). During the first 30 s starting from this initial condition, the phase portrait of the uncontrolled system is depicted in **Figure 5** in the phase plane $(X, \dot{x})$ which refers to the angle and angular velocity of the link, respectively. It can be seen from **Figure 5** that the ideal phase plane orbit of the giant swing motions traces out a closed curve.

To see the stability of periodic orbits via delayed feedback control, numerical simulation was exercised from the initial condition $x(0) = (\pi, 0.1, 9.252, -2.39)$ that contained errors. First, consider the uncontrolled case, the 30 s trajectory of the orbits in the phase plane filled up a section of the phase space as in **Figure 6**. It can be confirmed that there was no periodicity without control.

Next, consider the system controlled by the proposed method, with which the error transfer matrix A was obtained as follows:

$$A = \begin{bmatrix} 1.0054 & 0.0521 & 0.5986 & 0.0954 \\ -0.0377 & 0.7685 & -0.1017 & 0.0210 \\ 0.2982 & 1.8534 & 1.0041 & 0.0399 \\ -1.7310 & -10.6479 & -0.0170 & 0.7728 \end{bmatrix}.$$

The input matrix B in the case of $\tau = 10$(ms) is obtained as follows:

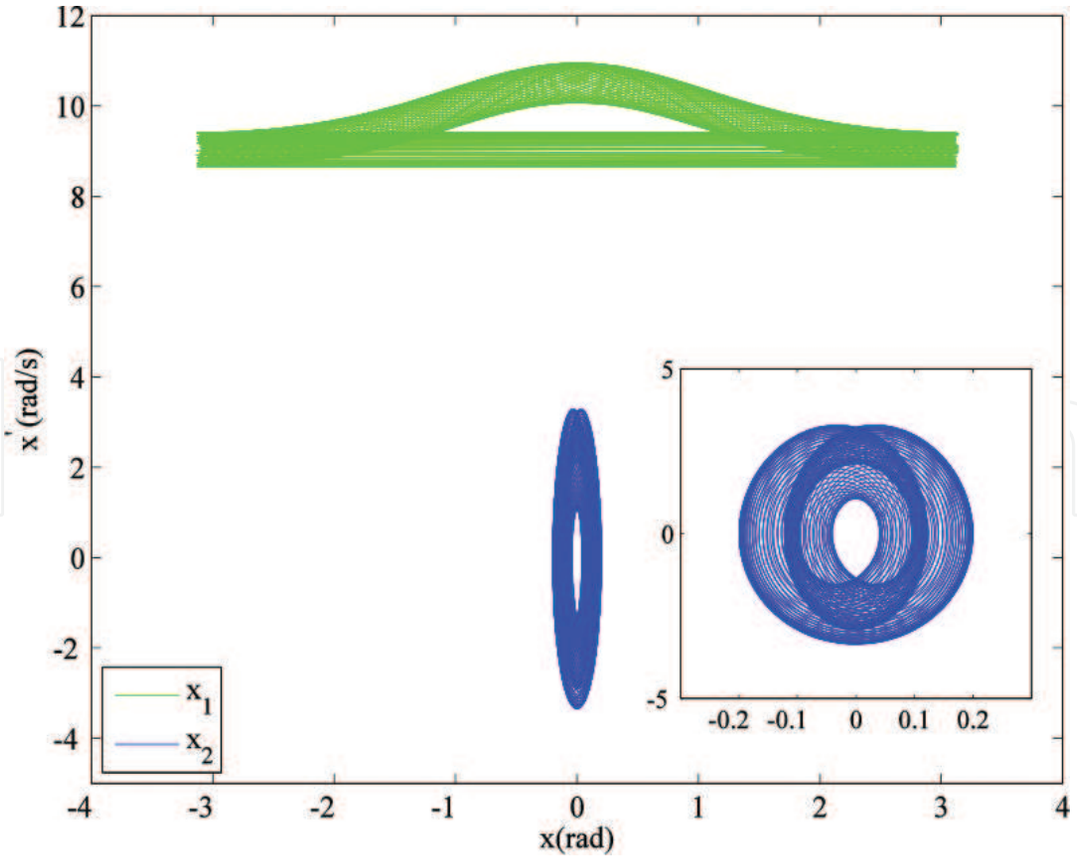

Figure 6. Phase portrait of X–$\dot{x}$ (with error).

http://dx.doi.org/10.5772/65831

$$B = \begin{bmatrix} -0.000167 \\ 0.000552 \\ -0.004464 \\ 0.024859 \end{bmatrix}.$$

Based on the value of the matrix A and B shown in the above, the feedback gain K was obtained by assigning all of its poles of the system matrix $A + B\widehat{K}$ in the unit disk. Generally, in a linear system, the poles of the system matrix $A + B\widehat{K}$ are assigned as close as possible to the origin in order to decrease the convergence time; however, in such a nonlinear system as gymnastic robot, it is found that it becomes to show the divergence while the poles of $A + B\widehat{K}$ is in the disk with ratio equals 0.6 approximately. Here, two cases were studied by assigning the poles larger than 0.6 as follows.

$$\begin{cases} Case\ I: & pole = (0.75, 0.73, 0.71, 0.69), & K = (-2242.7, -128.82, 48526, 8447.7), \\ Case\ II: & pole = (0.90, 0.88, 0.835, 0.815), & K = (-206.94, 354.01, 1577.1, 296.42). \end{cases}$$

In Case I, the numerical simulation results via calculated feedback gain K are shown in **Figure 7**. **Figure 7(a)** and **(b)** show the trajectory of the orbits in the phase plane $(x, \dot{x})$, of which **Figure 7(a)** depicts the trajectory of the first 50 s, while **Figure 7(b)** plots that of 50 ~ 60

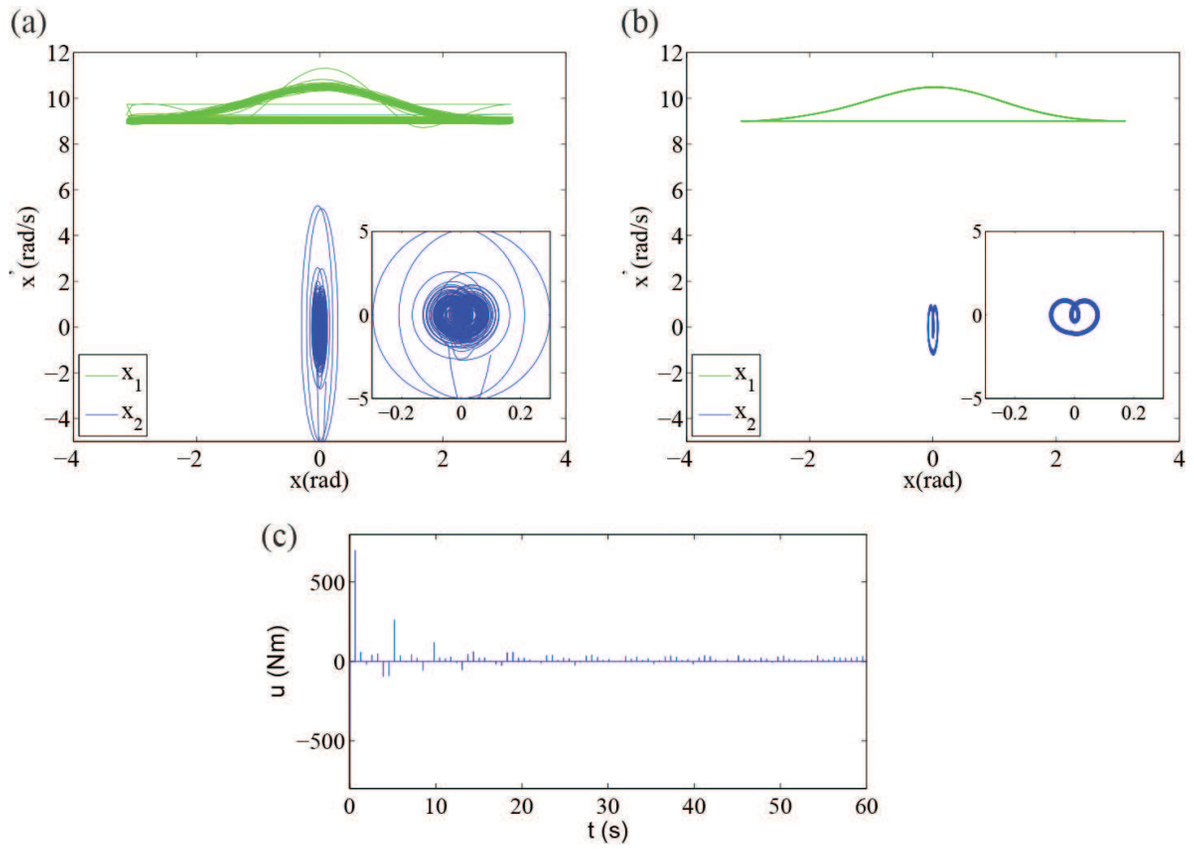

Figure 7. Phase portrait and joint torque (Case I): (a) Phase portrait of X–$\dot{x}$(t=0~50s); (b) Phase portrait of X–$\dot{x}$ (t=50~60s); (c) Joint torque.

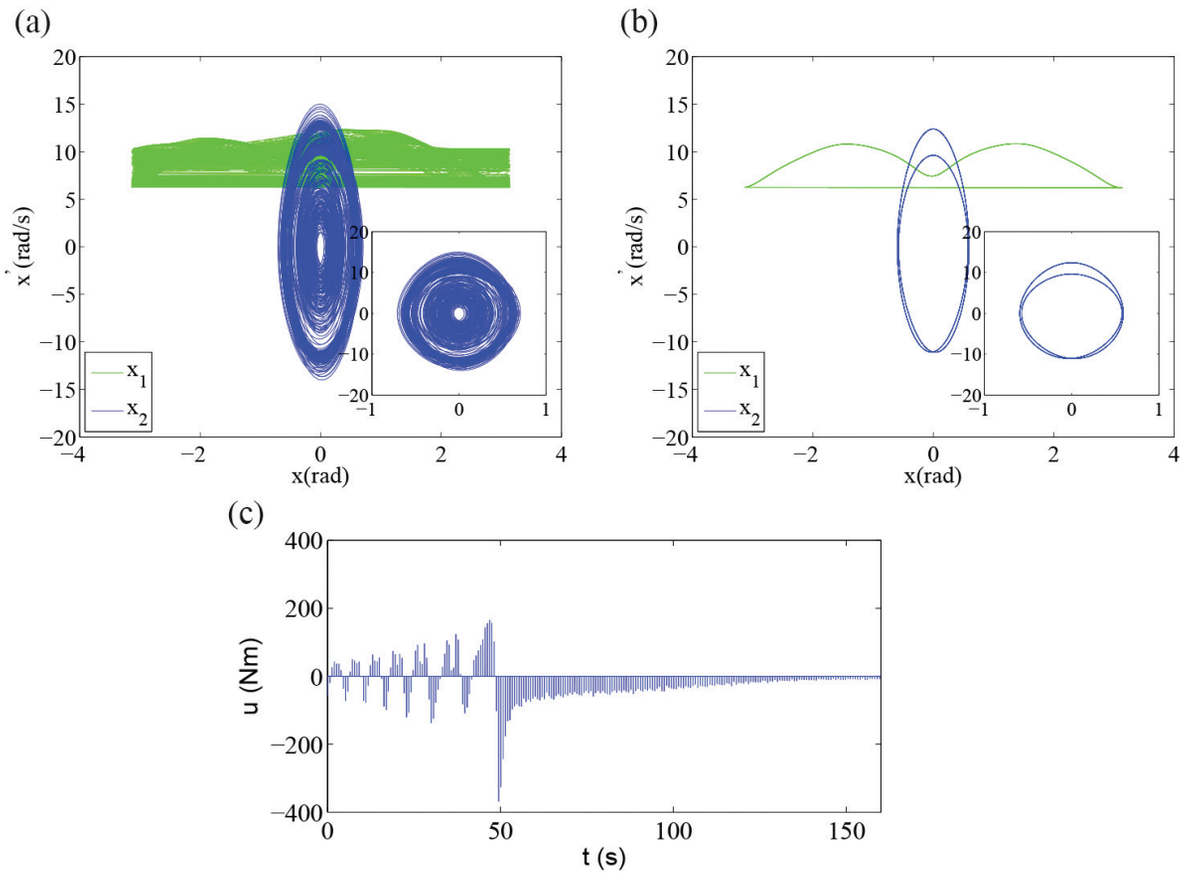

Figure 8. Phase portrait and joint torque (Case II): (a) Phase portrait of X–$\dot{x}$ (t=0~150s); (b) Phase portrait of X–$\dot{x}$ (t=150~160s); (c) Joint torque.

(s). Meanwhile, the time history of control input is shown in **Figure 7(c)** from which it can be seen that the control input diminished with time. It is obvious that from **Figure 7(c)**, the control input u began to vanish from about t = 30(s), and from **Figure 7(b)** the periodicity began to appear from approximately t = 50(s).

However, on further analysis conducted, it was found that one can change the type of giant swing type by changing the pole placement of the matrix $A + B\widehat{K}$. This phenomenon is shown in **Figure 8** which depicts the change histories of link angle, angular velocity, and input control with 160 s in Case II. The first 150 s trajectory of the orbits in the phase plane (x, $\dot{x}$) is depicted in **Figure 8(a)** and the remaining is shown in **Figure 8(b)**. Moreover, the time history of input torque is shown in **Figure 8(c)**.

It could be said that in Case II, the proposed method showed the ability of controlling the giant-swing motion to an unknown periodic orbit, which is known as one of the advantages of delayed feedback control.

Moreover, **Figures 9** and **10** depict the stick diagrams based on one period data after the giant swing motion converging to a stable orbit in Case I and Case II, in which the figures of (a), (b),

http://dx.doi.org/10.5772/65831

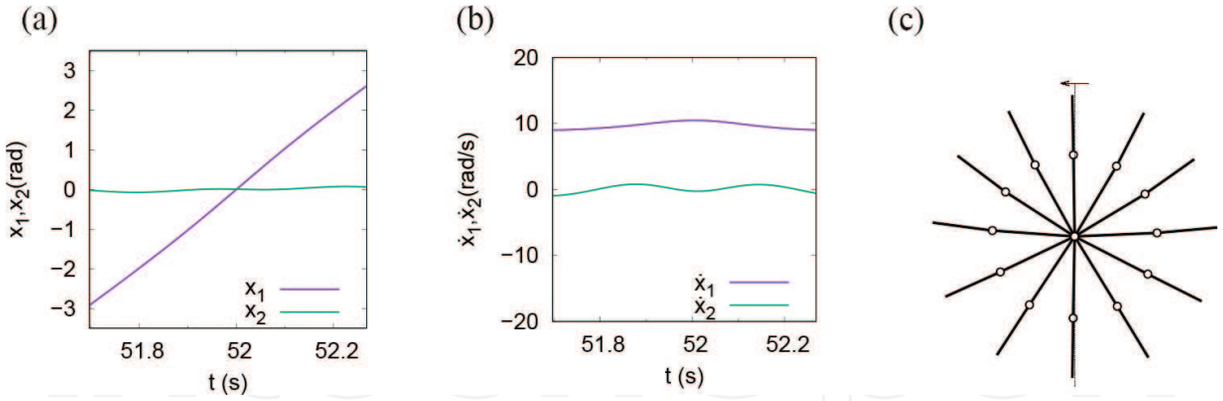

Figure 9. Angle, angular velocity, and stick (Case I).

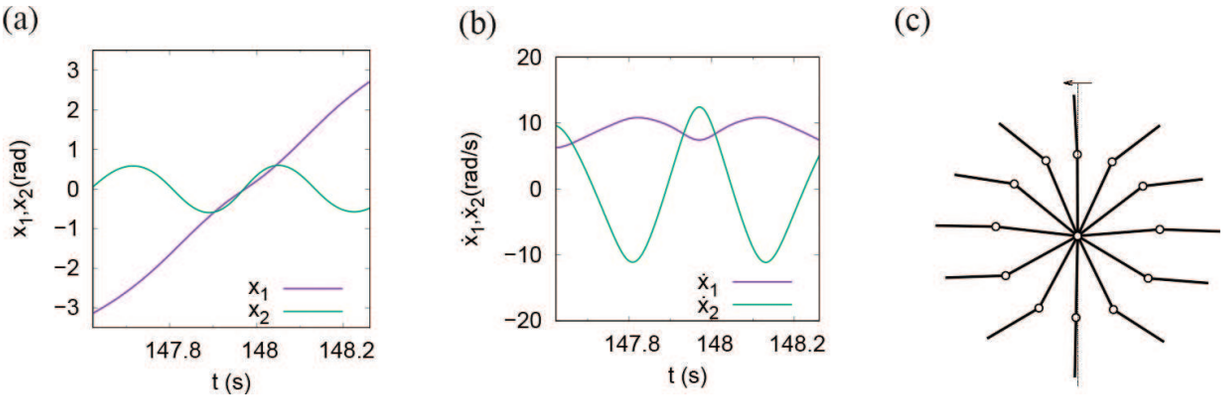

Figure 10. Angle, angular velocity, and stick (Case II).

and (c) plot, respectively, the angle, angular velocity, and stick figure. From the above two figures, it can be seen that the difference between the assigned poles caused periodic giant swing motion to change to a different type.

5. Conclusion

This chapter studied the behavior of the giant swing motions of a two-link and a four-link horizontal bar gymnastic robot systems via delayed feedback control. First, it has been discussed as a solution to calculate analytically the error transfer matrix and the input matrix by which the stability of DFC for the original two-link gymnastic robot system is equivalent to that of the corresponding discrete system. Moreover, it was introduced as a method by which a feedback gain to ensure the stability of original system can be determined. Second, a modified DFC method, MDFC, has been extended to a four-link gymnastic robot. Plural Poincaré maps were defined so that the stability of the close-loop system can be evaluated based on the theory of monodromy matrix. Finally, the simulation results showed its effectiveness.

Acknowledgments

This work is supported in part by the Project Sponsored by the Scientific Research Foundation for the Returned Overseas Chinese Scholars, State Education Ministry, and in part by the Scientific Research Foundation for Young Teachers, Shanghai JiaoTong University.

Author details

Dasheng Liu

Address all correspondence to: dsliu@sjtu.edu.cn

Department of Instrument Science and Engineering, School of Electronic Information and Electrical Engineering, Shanghai JiaoTong University, Shanghai, China

References

[1] E. N. Lorenz. Deterministic nonperiodic flow. *Journal of the Atmospheric Sciences*, 20:130–141, 1963.

[2] R. M. May. Simple mathematical models with very complicated dynamics. *Nature*, 261:459–467, 1976.

[3] W. Charlotte. What are the new implications of chaos for unpredictability? *The British Journal for the Philosophy of Science*, 60:195–220, 2009.

[4] S. Boccaletti, C. Grebogi, Y. C. Lai, H. Mancini, and D. Maza. The control of chaos: theory and applications. *Physics Reports*, 329(3):103–197, 2000.

[5] F. T. Arecchi, S. Boccaletti, M. Ciofini, R. Meucci, and R. Meucci. The control of chaos: theoretical schemes and experimental realizations. *International Journal of Bifurcation and Chaos*, 8(8):1643–1655, 1998.

[6] E. Ott, C. Grebogi, and J. A. Yorke. Controlling chaos. *Physical Review Letters*, 64(11):1196–1199, 1990.

[7] K. Pyragas. Continuous control of chaos by self-controlling feedback. *Physics Letters A*, 170(6):421–428, 1992.

[8] K. Pyragas. Control of chaos via extended delay feedback. *Physics Letters A*, 206(5–6):323–330, 1995.

[9] M. E. Bleich and J. E. S. Socolar. Stability of periodic orbits controlled by time-delay feedback. *Physics Letters A*, 210(1–2):87–94, 1996.

[10] S. Rajasekar, K. Murali, and M. Lakshmanan. Control of chaos by nonfeedback methods in a simple electronic circuit system and the Fitzhugh-Nagumo equation. *Chaos, Solitons and Fractals*, 8:1545–1558, 1997.

[11] A. Zhalnin. Control of chaos in nonautonomous systems with quasiperiodic excitation. *Technical Physics Letters*, 25:662–664, 1999. DOI:10.1134/1.1262590.

[12] P. J. Aston and C. M. Bird. Using control of chaos to refine approximations to periodic points. *International Journal of Bifurcation & Chaos*, 10:227–235, 2000.

[13] M. Basso, R. Genesio, and A. Tesi. Stabilizing periodic orbits of forced systems via generalized pyragas controllers. *IEEE Transactions on Circuits and Systems I: Fundamental Theory and Applications*, 44(10):1023–1027, 1997.

[14] K. Pyragas. Control of chaos via an unstable delayed feedback controller. *Physical Review Letters*, 86(11):2265–2268, 2001.

[15] Y. P. Tian. Controlling chaos using invariant manifolds. *International Journal of Control*, 72:258–266, 1999.

[16] F. T. Arecchi and S. Boccaletti. Adaptive strategies for recognition, noise filtering, control, synchronization and targeting of chaos. *Chaos*, 7:621–634, 1997.

[17] K. Konishi and H. Kokame. Observer-based delayed-feedback control for discrete-time chaotic systems. *Physics Letters A*, 248(5–6):359–368, 1998.

[18] T-D Eom, M Sugisaka, and J-J Lee. New skill learning paradigm using various kinds of neurons. *Applied Mathematics and Computation*, 91(1):9–22, 1998.

[19] O. Calvo and J. H. E. Cartwright. Fuzzy control of chaos. *International Journal of Bifurcation and Chaos*, 8(8):1743–1747, 1998.

[20] T Useo and S Yamamoto. A generalization of delayed feedback control in chaotic discrete-time systems. *IEICE Technical Report. Nonlinear Problems*: *The Institute of Electronics, Information and Communication Engineers*, 97(592):17–22, 1998. (In Japanese.)

[21] S. Mizutani, T. Sano, T. Uchiyama, and N. Sonehara. Controlling chaos in chaotic neural networks. *IEICE Technical Report*. *Nonlinear Problems*: *The Institute of Electronics, Information and Communication Engineers*, 95(47):41–48, 1995. (In Japanese.)

[22] A. L. Fradkov and R. J. Evans. Control of chaos: methods and applications in engineering. *Annual Reviews in Control*, 29(1):33–56, 2005.

[23] E. Scholl, K. Pyragas, D. Cooper, and R. Dottling. Tuning of semiconductor oscillators by chaos control. *Semiconductor Science and Technology*, 9(5):559–563, 1994.

[24] T. Hikihara and T. Kawagoshi. An experimental study on stabilization of unstable periodic motion in magneto-elastic chaos. *Physics Letters A*, 211(1):29–36, 1996.

[25] Y. Nakamura, T. Suzuki, and M. Koinuma. Nonlinear behavior and control of a nonholonomic free-joint manipulator. *IEEE Transactions on Robotics and Automation*, 13 (6):853–862, 1997.

[26] S. Bielawski, M. Bouazaoui, D. Derozier, and P. Glorieux. Stabilization and characterization of unstable steady states in a laser. *Physical Review A*, 47(4):3276–3279, 1993.

[27] P. Parmananda, R. Madrigal, M. Rivera, L. Nyikos, I. Z. Kiss, and V. Gaspar. Stabilization of unstable steady states and periodic orbits in an electrochemical system using delayed-feedback control. *Physical Review E*, 59:5266–5271, 1999.

[28] H. Qammar, K. R. Seshadhri, R. Gomatam, and A. Venkatesan. Control of a chaotic polymerization reaction using linear and nonlinear controllers. *The Chemical Engineering Journal and the Biochemical Engineering Journal*, 64(1):141–148, 1996.

[29] J. A. Holyst and K. Urbanowicz. Chaos control in economical model by time-delayed feedback method. *Physica A: Statistical Mechanics and its Applications*, 287(3–4):587–598, 2000.

[30] A. Tamaševičius, G. Mykolaitis, V. Pyragas, and K. Pyragas. Delayed feedback control of periodic orbits without torsion in nonautonomous chaotic systems: theory and experiment. *Physical Review E*, 76(2):026203, 2007.

[31] M. Brucoli, D. Cafagna, L. Carnimeo, and G. Grassi. Synchronization of hyperchaotic circuits via continuous feedback control with application to secure communications. *International Journal of Bifurcation & Chaos*, 8:2031–2040, 1998.

[32] A. Sano. Dynamic biped walking by using skillfully a gravity field (challenge to a human walking). *Journal of the Robotics Society of Japan*, 11(3):52–57, 1993. (In Japanese.)

[33] K. Ono, R. Takahashi, A. Imadu, and T. Shimada. Self-excitation control for biped walking mechanism, Proceedings of the 2000 IEEE/RSJ Int. Conf. on Intelligent Robots and Systems, pp. 1149–1154.

[34] J. Nakanishi, T. Fukuda, and D. E. Koditschek. Study on the control of a two-link brachiating robot: brachiation on a ladder with irregular intervals via target dynamics. *Transactions of the Japan Society of Mechanical Engineers. C*, 65(639):4387–4394, 1999. (In Japanese.)

[35] H. Nishimura, K. Takasaki, K. Funaki, and T. Totani. Motion control of brachiation robot by means of final-state control with error learning. *Transactions of the Japan Society of Mechanical Engineers. C*, 63(605):182–189, 1997. (In Japanese.)

[36] S. Takashima. A robot performing gymnastics on the bar. *Journal of the Society of Biomechanisms*, 15(4):190–197, 1991. (In Japanese.)

[37] M. W. Spong. The swing up control problem for the actobot. *IEEE Control Systems*, 15:49–55, 1995.

[38] A. Imadu and K. Ono. Optimum trajectory planning method for a system that includes passive joints: 1st report, proposal of a function approximation method. *Transactions of the Japan Society of Mechanical Engineers*. *C*, 64(618):516–522, 1998. (In Japanese.)

[39] A. Imadu, K. Ono, and K. Yamamoto. Optimum trajectory planning method for a system that includes passive joints: 2nd report, analysis of the giant swing motions and their systematic search method based on optimum trajectory planning. *Transactions of the Japan Society of Mechanical Engineers*. *C*, 65(637):3583–3591, 1999. (In Japanese.)

[40] N. Ogino, H. Kinjo, E. Uezato, and T. Yamamoto. Design of nonholonomic control system using neuro controller evolved by GA training. *IEICE Technical Report*. *Neurocomputing*: *The Institute of Electronics*, *Information and Communication Engineers*, 105(131):41–44, 2005. (In Japanese.)

[41] M. Sampei. Vehicle control and nonlinear control theory: Control for nonholonomic systems. *The Transactions of the Institute of Electrical Engineers of Japan*. *D*, *A Publication of Industry Applications Society*, 114(10):955–958, 1994. (In Japanese.)

[42] K. Senda, Y. Murotsu, and M. Ozaki. A method of attitude control for space robots: an approach using a neural network. *Transactions of the Japan Society of Mechanical Engineers*. *C*, 57(539):2356–2362, 1991. (In Japanese.)

[43] Y. Nakamura, M. Koinuma, and T. Suzuki. Chaotic behavior and nonlinear control of a two-joint planer arm with a free joint-control of nonholonomic mechanisms with drift. *Journal of the Robotics Society of Japan*, 14(4):602–611, 1996. (In Japanese.)

[44] H. Arai. Nonholonomic control of underactuated manipulators. *Systems*, *Control and Information*: *Journal of the Institute of Systems*, *Control and Information Engineers*, 43 (10):553–560, 1999. (In Japanese).

[45] A. Imadu, K. Yamamoto, and K. Ono. Analysis of free giant swing motions of a 2-DOF link mechanism. *Transactions of the Japan Society of Mechanical Engineers*. *C*, 66(644):1102–1109, 2000. (In Japanese.)

[46] K. Yamamoto, K. Ono, and A. Imadu. Control of giant swing motions of a 2-DOF link mechanism. *Transactions of the Japan Society of Mechanical Engineers*. *C*, 66(651):3591–3599, 2000. (In Japanese.)

[47] H. Yamaura, K. Ono, and H. Suzuki. Giant-swing motions of a 3-DOF link mechanism. *Dynamics and Design Conference*: *Proceedings of Dynamics*, *Measurement and Control*: *D*, 2002:150, 2002. (In Japanese.)

[48] H. Yamaura, H. Suzuki, and K. Ono. Giant-swing motions and control of a 3-DOF link mechanism. *Transactions of the Japan Society of Mechanical Engineers*. *C*, 71(707):2289–2296, 2005. (In Japanese.)

[49] H. Yamaura and M. Yanai. A realization method of giant-swing motion of 3-DOF link mechanism. *Transactions of the Japan Society of Mechanical Engineers*. *C*, 72(721):2812–2820, 2006. (In Japanese.)

[50] D. Liu and H. Yamaura. Realization of Giant Swing Motions of a two-link horizontal bar gymnastic robot Using Delayed Feedback Control, Transactions of the Japan Society of Mechanical Engineers, 76-767, C(2010), pp.1700–1707. (In Japanese)

[51] D. Liu and H. Yamaura. Stabilization control for giant swing motions of 3-link horizontal bar gymnastic robot using multiple-prediction delayed feedback control with a periodic gain. *Journal of System Design and Dynamics*, 5:42–54, 2011.

[52] K. Ono, A. Imadu, and T. Sakai. Optimal motion trajectory of giant swing. *Transactions of the Japan Society of Mechanical Engineers*. *C*, 62(599):2640–2647, 1996. (In Japanese.)